

Near-infrared trapped mode magnetic resonance in an all-dielectric metamaterial

Jianfa Zhang,¹ Kevin F. MacDonald,^{1*} and Nikolay I. Zheludev^{1,2}

¹Optoelectronics Research Centre & Centre for Photonic Metamaterials, University of Southampton, Highfield, Southampton, SO17 1BJ, UK

²Centre for Disruptive Photonic Technologies, Nanyang Technological University, Singapore 637371, Singapore

*kfm@orc.soton.ac.uk

<http://www.metamaterials.org.uk>

Abstract: Optical responses in conventional metamaterials based on plasmonic metal nanostructures are inevitably accompanied by Joule losses, which obstruct practical applications by limiting resonance quality factors and compromising the efficiency of metamaterial devices. Here we experimentally demonstrate a fully-dielectric metamaterial that exhibits a ‘trapped mode’ resonance at optical frequencies, founded upon the excitation by incident light of anti-parallel displacement currents in meta-molecules comprising pairs of parallel, geometrically dissimilar dielectric nano-bars. The phenomenon is demonstrated in the near-infrared part of the spectrum using silicon, showing that in principle strong, lossless resonant responses are possible anywhere in the optical spectral range.

©2013 Optical Society of America

OCIS codes: (160.3918) Metamaterials; (310.6628) Subwavelength structures, nanostructures; (160.4760) Optical properties.

References and links

1. C. M. Soukoulis and M. Wegener, “Past achievements and future challenges in the development of three-dimensional photonic metamaterials,” *Nat. Photonics* **5**, 523–530 (2011).
2. N. I. Zheludev and Y. S. Kivshar, “From metamaterials to metadevices,” *Nat. Mater.* **11**(11), 917–924 (2012).
3. D. R. Smith, J. B. Pendry, and M. C. K. Wiltshire, “Metamaterials and negative refractive index,” *Science* **305**(5685), 788–792 (2004).
4. V. M. Shalaev, “Optical negative-index metamaterials,” *Nat. Photonics* **1**(1), 41–48 (2007).
5. S. P. Burgos, R. de Waele, A. Polman, and H. A. Atwater, “A single-layer wide-angle negative-index metamaterial at visible frequencies,” *Nat. Mater.* **9**(5), 407–412 (2010).
6. T. Xu, A. Agrawal, M. Abashin, K. J. Chau, and H. J. Lezec, “All-angle negative refraction and active flat lensing of ultraviolet light,” *Nature* **497**(7450), 470–474 (2013).
7. K. Aydin, V. E. Ferry, R. M. Briggs, and H. A. Atwater, “Broadband polarization-independent resonant light absorption using ultrathin plasmonic super absorbers,” *Nat Commun* **2**, 517 (2011).
8. C. Wu, B. Neuner III, J. John, A. Milder, B. Zollars, S. Savoy, and G. Shvets, “Metamaterial-based integrated plasmonic absorber/emitter for solar thermo-photovoltaic systems,” *J. Opt.* **14**(2), 024005 (2012).
9. B. Gholipour, J. Zhang, K. F. MacDonald, D. W. Hewak, and N. I. Zheludev, “An all-optical, non-volatile, bidirectional, phase-change meta-switch,” *Adv. Mater.* **25**(22), 3050–3054 (2013).
10. J. Zhang, K. F. MacDonald, and N. I. Zheludev, “Controlling light-with-light without nonlinearity,” *Light Sci. App.* **1**(7), e18 (2012).
11. E. Hendry, T. Carpy, J. Johnston, M. Popland, R. V. Mikhaylovskiy, A. J. Laphorn, S. M. Kelly, L. D. Barron, N. Gadegaard, and M. Kadodwala, “Ultrasensitive detection and characterization of biomolecules using superchiral fields,” *Nat. Nanotechnol.* **5**(11), 783–787 (2010).
12. E. Plum, V. A. Fedotov, P. Kuo, D. P. Tsai, and N. I. Zheludev, “Towards the lasing spaser: controlling metamaterial optical response with semiconductor quantum dots,” *Opt. Express* **17**(10), 8548–8551 (2009).
13. Z. G. Dong, H. Liu, T. Li, Z. H. Zhu, S. M. Wang, J.-X. Cao, S.-N. Zhu, and X. Zhang, “Optical loss compensation in a bulk left-handed metamaterial by the gain in quantum dots,” *Appl. Phys. Lett.* **96**(4), 044104 (2010).
14. S. Xiao, V. P. Drachev, A. V. Kildishev, X. Ni, U. K. Chettiar, H. K. Yuan, and V. M. Shalaev, “Loss-free and active optical negative-index metamaterials,” *Nature* **466**(7307), 735–738 (2010).
15. A. Boltasseva and H. A. Atwater, “Low-loss plasmonic metamaterials,” *Science* **331**(6015), 290–291 (2011).
16. J. A. Schuller, R. Zia, T. Taubner, and M. L. Brongersma, “Dielectric metamaterials based on electric and magnetic resonances of silicon carbide particles,” *Phys. Rev. Lett.* **99**(10), 107401 (2007).

17. K. Vynck, D. Felbacq, E. Centeno, A. I. Căbuz, D. Cassagne, and B. Guizal, "All-dielectric rod-type metamaterials at optical frequencies," *Phys. Rev. Lett.* **102**(13), 133901 (2009).
18. A. García-Etxarri, R. Gómez-Medina, L. S. Froufe-Pérez, C. López, L. Chantada, F. Scheffold, J. Aizpurua, M. Nieto-Vesperinas, and J. J. Sáenz, "Strong magnetic response of submicron silicon particles in the infrared," *Opt. Express* **19**(6), 4815–4826 (2011).
19. L. Shi, T. U. Tuzer, R. Fenollosa, and F. Meseguer, "A new dielectric metamaterial building block with a strong magnetic response in the sub-1.5-micrometer region: silicon colloid nanocavities," *Adv. Mater.* **24**(44), 5934–5938 (2012).
20. A. I. Kuznetsov, A. E. Miroshnichenko, Y. H. Fu, J. B. Zhang, and B. S. Luk'yanchuk, "Magnetic light," *Sci Rep* **2**, 492 (2012).
21. A. B. Evlyukhin, S. M. Novikov, U. Zywietz, R. L. Eriksen, C. Reinhardt, S. I. Bozhevolnyi, and B. N. Chichkov, "Demonstration of magnetic dipole resonances of dielectric nanospheres in the visible region," *Nano Lett.* **12**(7), 3749–3755 (2012).
22. L. Peng, L. Ran, H. Chen, H. Zhang, J. A. Kong, and T. M. Grzegorzczuk, "Experimental observation of left-handed behavior in an array of standard dielectric resonators," *Phys. Rev. Lett.* **98**(15), 157403 (2007).
23. B. I. Popa and S. A. Cummer, "Compact dielectric particles as a building block for low-loss magnetic metamaterials," *Phys. Rev. Lett.* **100**(20), 207401 (2008).
24. Q. Zhao, J. Zhou, F. Zhang, and D. Lippens, "Mie resonance-based dielectric metamaterials," *Mater. Today* **12**(12), 60–69 (2009).
25. J. C. Ginn, I. Brener, D. W. Peters, J. R. Wendt, J. O. Stevens, P. F. Hines, L. I. Basilio, L. K. Warne, J. F. Ihlefeld, P. G. Clem, and M. B. Sinclair, "Realizing optical magnetism from dielectric metamaterials," *Phys. Rev. Lett.* **108**(9), 097402 (2012).
26. S. Liu, J. F. Ihlefeld, J. Dominguez, E. F. Gonzales, J. E. Bower, D. B. Burckel, M. B. Sinclair, and I. Brener, "Realization of tellurium-based all dielectric optical metamaterials using a multi-cycle deposition-etch process," *Appl. Phys. Lett.* **102**(16), 161905 (2013).
27. L. Shi, J. T. Harris, R. Fenollosa, I. Rodriguez, X. Lu, B. A. Korgel, and F. Meseguer, "Monodisperse silicon nanocavities and photonic crystals with magnetic response in the optical region," *Nat Commun* **4**, 1904 (2013).
28. V. A. Fedotov, M. Rose, S. L. Prosvirnin, N. Papasimakis, and N. I. Zheludev, "Sharp trapped-mode resonances in planar metamaterials with a broken structural symmetry," *Phys. Rev. Lett.* **99**(14), 147401 (2007).
29. V. V. Khardikov, E. O. Iarko, and S. L. Prosvirnin, "A giant red shift and enhancement of the light confinement in a planar array of dielectric bars," *J. Opt.* **14**(3), 035103 (2012).
30. N. Katsarakis, T. Koschny, M. Kafesaki, E. N. Economou, and C. M. Soukoulis, "Electric coupling to the magnetic resonance of split ring resonators," *Appl. Phys. Lett.* **84**(15), 2943–2945 (2004).
31. B. S. Luk'yanchuk, N. I. Zheludev, S. A. Maier, N. J. Halas, P. Nordlander, H. Giessen, and C. T. Chong, "The Fano resonance in plasmonic nanostructures and metamaterials," *Nat. Mater.* **9**(9), 707–715 (2010).
32. T. Koschny, P. Markoš, D. R. Smith, and C. M. Soukoulis, "Resonant and antiresonant frequency dependence of the effective parameters of metamaterials," *Phys. Rev. E Stat. Nonlin. Soft Matter Phys.* **68**(6), 065602 (2003).
33. R. Liu, T. J. Cui, D. Huang, B. Zhao, and D. R. Smith, "Description and explanation of electromagnetic behaviors in artificial metamaterials based on effective medium theory," *Phys. Rev. E Stat. Nonlin. Soft Matter Phys.* **76**(2), 026606 (2007).
34. K. Hennessy, A. Badolato, M. Winger, D. Gerace, M. Atatüre, S. Gulde, S. Fält, E. L. Hu, and A. Imamoglu, "Quantum nature of a strongly coupled single quantum dot-cavity system," *Nature* **445**(7130), 896–899 (2007).
35. K. Tanaka, E. Plum, J. Y. Ou, T. Uchino, and N. I. Zheludev, "Multifold enhancement of quantum dot luminescence in plasmonic metamaterials," *Phys. Rev. Lett.* **105**(22), 227403 (2010).
36. N. I. Zheludev, S. L. Prosvirnin, N. Papasimakis, and V. A. Fedotov, "Lasing spaser," *Nat. Photonics* **2**(6), 351–354 (2008).
37. J. Zhang, K. F. MacDonald, and N. I. Zheludev, "Nonlinear dielectric optomechanical metamaterials," *Light Sci. App.* **2**(8), e96 (2013).

For a decade and more, considerable effort has been focused on the engineering of metamaterials - the advancement of fundamental theory and of computational and fabrication techniques [1, 2] - to achieve high-quality resonant responses at technologically-relevant near-infrared and visible wavelengths for applications ranging from negative refraction [3–6] to photovoltaic power generation, electro-/all-optical signal modulation/switching, and biosensing [7–11]. However, the vast majority of metamaterial structures employed here comprise arrays of sub-wavelength metallic (typically split-ring) resonators. These suffer from high inherent energy dissipation due to resistive losses in the metal, especially in the near-infrared to visible range, which severely compromise optical properties and limit potential applications. Numerous efforts have been made to incorporate gain media into metamaterials for loss compensation [12–14] but extremely high pump powers may be needed to compensate the large losses and would unavoidably introduce significant noise and heat.

Consequently, there has been growing interest in the development and application of low loss alternatives to metals as plasmonic media [15].

Recently, the Mie resonances of dielectric particles have been proposed as a platform for the engineering of magnetic resonances [16–21], and on this basis magnetic responses have been experimentally realized in metamaterials and photonic crystals fabricated from high permittivity dielectrics such as titanium dioxide and germanium, at microwave and terahertz frequencies [22–24] and more recently in the infrared/optical range [25–27]. Here we experimentally demonstrate another mechanism via which strong visible and near-infrared resonances can be achieved in purely dielectric metamaterials: A magnetic resonance akin to the well-known ‘trapped mode’ of metallic asymmetric split ring (ASR) structures [28] is realized through a coupling between closely spaced, dissimilar dielectric nano-bars within the metamaterial unit cell [29]. These trapped modes are characterized by anti-phased oscillation in the two arms of the unit cell of conduction current / surface plasmon-polariton excitations in metals, or displacement currents in dielectric structures as illustrated schematically in Fig. 1. The scattered electromagnetic fields generated by such current configurations are very weak, with both electric and magnetic dipole radiation components being cancelled via destructive interference. This dramatically reduces coupling to free space and therefore radiation losses. Excitation of such modes relies critically on structural symmetry breaking.

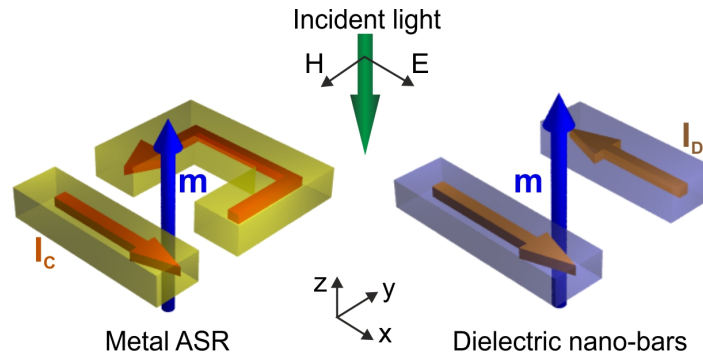


Fig. 1. Analogous trapped mode resonances in metallic (left) and dielectric (right) metamaterials (a single sub-wavelength, asymmetric unit resonator of each type being shown) based on the anti-phase oscillation of conduction or displacement currents and consequential excitation of out-of-plane magnetic moments.

Low-loss media with high refractive indices must be used as a platform for the assembly of dielectric metamaterials in order to minimize absorption losses while ensuring that the metamaterial unit cells are effectively of sub-wavelength size to exclude diffraction effects. Semiconductors such as silicon, germanium, and tellurium are among the best candidates due to their high refractive indices (>3) and relatively low absorption in the optical range. The present study employs silicon, which has a bandgap of 1.1 eV, a refractive index of around 3.5 and low absorption in the near-IR telecommunications wavelength range (see Fig. 2). 160 nm thick amorphous films are deposited by plasma-enhanced chemical vapor deposition (PECVD) at 250°C on glass substrates.

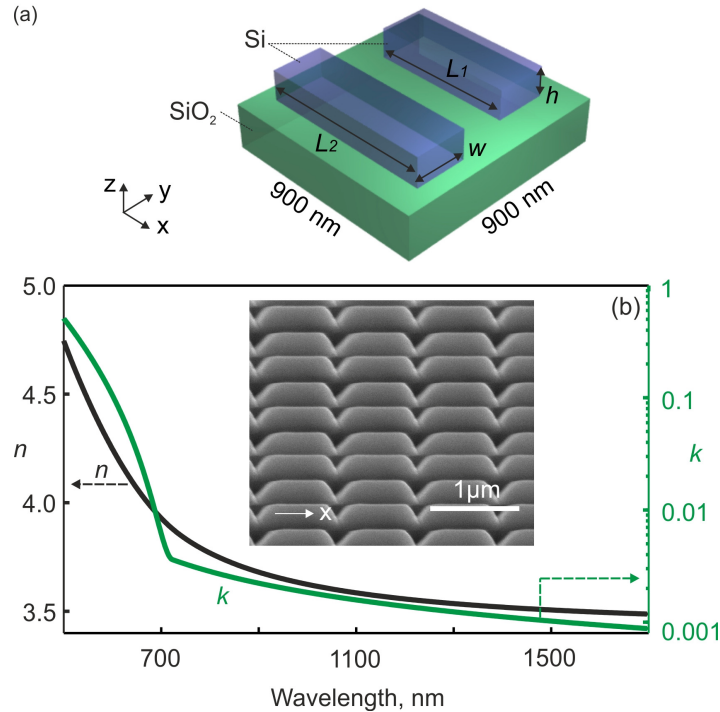


Fig. 2. All-dielectric Photonic Metamaterial: (a) Dimensional schematic of a unit cell of an all-dielectric metamaterial, comprising asymmetric silicon nano-bar pairs on silica, which exhibits sharp visible to near-IR 'trapped mode' magnetic resonances [$h = 160$, $w = 300$, $L_1 = 650$, $L_2 = 750$ nm]. The inset to part (b) shows a scanning electron microscope image of the experimental implementation of this design on a 160 nm amorphous silicon film (viewed at an oblique angle to the surface normal; full array size $30 \mu\text{m} \times 30 \mu\text{m}$). (b) Refractive index of unstructured PECVD amorphous silicon obtained via spectroscopic ellipsometry.

Dielectric metamaterial structures are then fabricated on these films by focused ion beam (FIB) milling on the basis of the 900 nm square unit cell design illustrated schematically in Fig. 2(a). Each cell contains a dissimilar pair of silicon bars with the same height (the 160 nm thickness of the Si film) and width (300 nm) but different lengths (nominally 650 and 750 nm). The ideal rectangular geometry of Fig. 2(a) is not translated flawlessly to experimental samples, such as shown inset to Fig. 2(b), but the observed imperfections are not found to compromise the essential nature of the metamaterial's resonant response.

Figure 3 shows measured normal-incidence optical transmission, reflection and absorption spectra for the metamaterial sample introduced in Fig. 2. A pronounced resonance is seen at a wavelength of around 1700 nm for incident light polarized (i.e. with electric field) parallel to the long (x) axes of the silicon nano-bars (solid lines in Figs. 3(a)-3(c)). For y -polarized light (i.e. incident with electric field perpendicular to the long axes of the dielectric bars), the sample's background level of transmission is somewhat higher, reflection somewhat lower and absorption slightly lower than for the x -polarization, but no resonance features are observed within the measured spectral range. For comparison, x -polarization data are also presented for a 'symmetric' control sample in which each unit cell contains two identical 700 nm long silicon bars (160 nm height, 300 nm width and 900 nm array period as for the asymmetric sample). The transmission, reflection and absorption levels here are broadly well-matched to those of the asymmetric sample for the same polarization, but the resonance features are, in keeping with the trapped mode's essential reliance on structural asymmetry, completely absent.

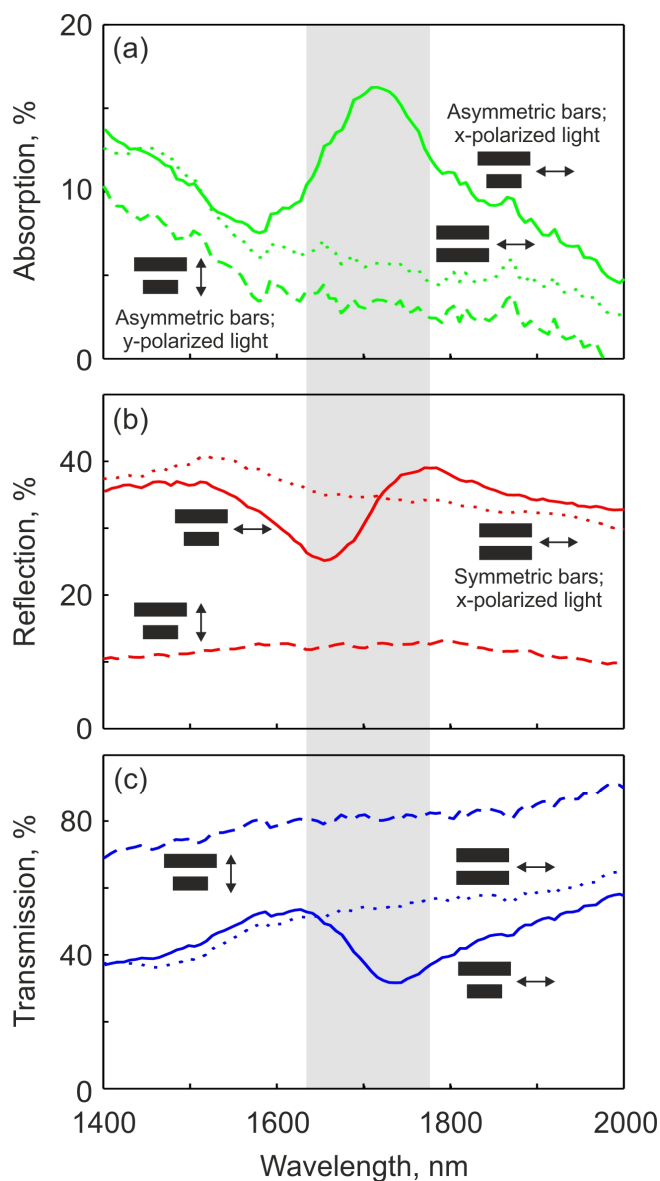


Fig. 3. Near-IR trapped mode resonance in an all-dielectric metamaterial. Absorption (a), reflection (b) and transmission (c) spectra, from microspectrophotometry measurements, for the silicon asymmetric nano-bar metamaterial structure shown in Fig. 2(b) under normally-incident illumination polarized in the x - and y -directions (respectively parallel and perpendicular to the long axes of the bars; plotted with solid and dashed lines), and for a symmetric control sample (all nano-bars of equal dimensions – dotted lines) under x -polarized light.

Important insight into the nature and origins of the resonance is provided by full-wave electromagnetic numerical simulations (performed using COMSOL MultiPhysics). Figure 4(a) presents simulated spectra for the sample design shown in Fig. 2(a) for normally incident x -polarized light. The calculations assume a silicon refractive index n_{Si} of 3.5, a substrate index of 1.46, zero absorption in both cases, and ideal rectangular cuboid Si bar shapes. As such the resonance features in the simulated spectra are very sharp, but otherwise (i.e. in terms of the trends in spectral dispersion) correlate well with the experimental data presented

in Fig. 3. Figure 2(b) illustrates that the zero-loss assumption is reasonable for an amorphous Si film in the wavelength range under consideration, and the glass substrate can also be considered lossless in this range. The damping of spectral resonance features observed in experiment is therefore attributed to manufacturing imperfections, specifically surface roughness (which introduces scattering losses), gallium contamination from the FIB milling process (introducing absorption), and cell-to-cell inhomogeneity across the array. Unlike their metallic (plasmonic) counterparts, dielectric metamaterials are largely insensitive to geometric complications at the scale of individual (sub-unit cell) elements [29], and indeed, in the present case modeling confirms that trapezoidal deviations from the ideal rectangular cuboid bar shape have little impact on resonance quality.

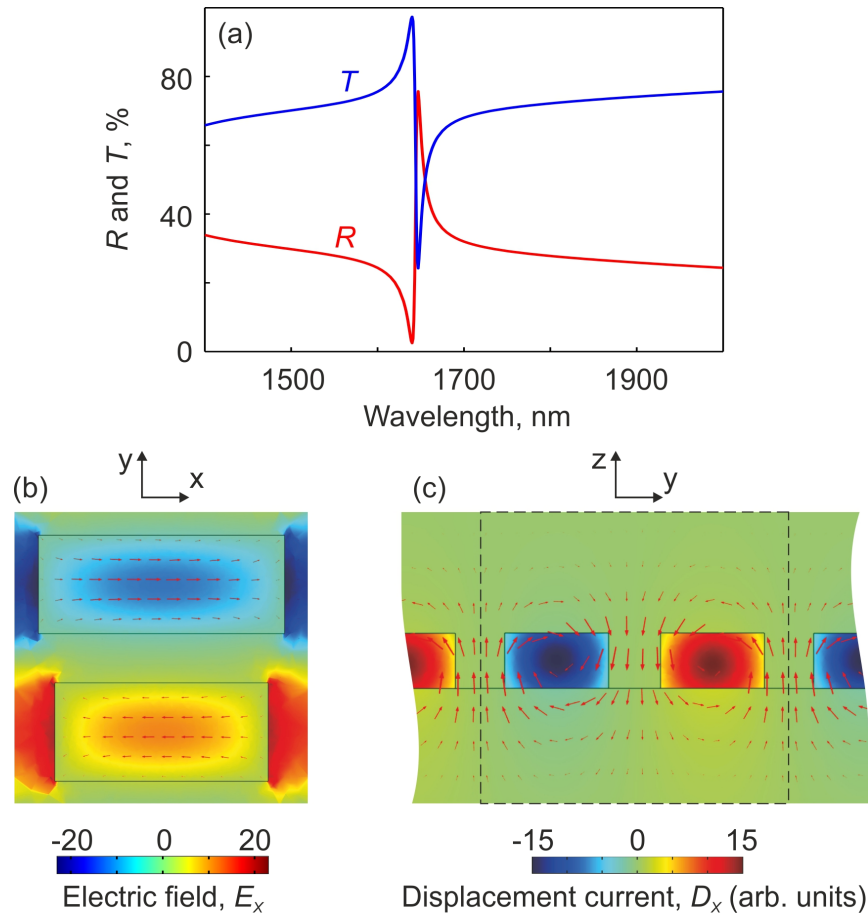


Fig. 4. Numerical modeling of near-IR dielectric metamaterials. (a) Simulated normal incidence x -polarization transmission and reflection spectra for a rectilinear metamaterial silicon-on-silica geometry based on the experimental sample design parameters shown in Fig. 2(a). (b) Magnitude of the x -component of electric field across an asymmetric Si nano-bar unit cell of the metamaterial structure at the resonance wavelength $\lambda_R = 1644$ nm, presented for the xy plane bisecting the nano-bars 80 nm above the substrate surface, overlaid with arrows indicating direction and magnitude of displacement current. (c) Corresponding magnitude of the x -component of displacement current presented for the yz symmetry plane of the unit cell, overlaid with arrows indicating direction and magnitude of magnetic field.

Figures 4(b) and 4(c) show cross-sections of the electric field distribution within a nano-bar pair unit cell of the metamaterial structure at the resonance wavelength. The two bars are excited in anti-phase, with electric polarizations of almost equal amplitude, and thereby display a magnetic mode resonance through electric coupling [30] – anti-parallel displacement

currents in the bars, indicated by the arrows overlaid in Fig. 4(b), generate an alternating ‘antiferromagnetic’ arrangement of out-of-plane magnetic moments, illustrated by the magnetic field arrows overlaid in Fig. 4(c). Similar resonances have been extensively studied in metallic planar metamaterials with a broken structural symmetry [28, 31].

As in metallic metamaterials composed of asymmetric split rings [28], the quality of trapped-mode resonances in dielectric metamaterials can be increased by reducing the asymmetry of the resonant elements. However, as the radiation losses are very low, losses are the limiting quantity on achievable quality factor Q ($= \lambda_r/\Delta\lambda$ where λ_r is the resonance frequency and $\Delta\lambda$ is the half-maximum linewidth) in such metamaterials. In Fig. 4(a), the quality factor of the trapped mode resonance is approximately 230. Figure 5 illustrates how this value decreases as losses, introduced via non-zero values for the imaginary part of the assumed silicon refractive index, increase.

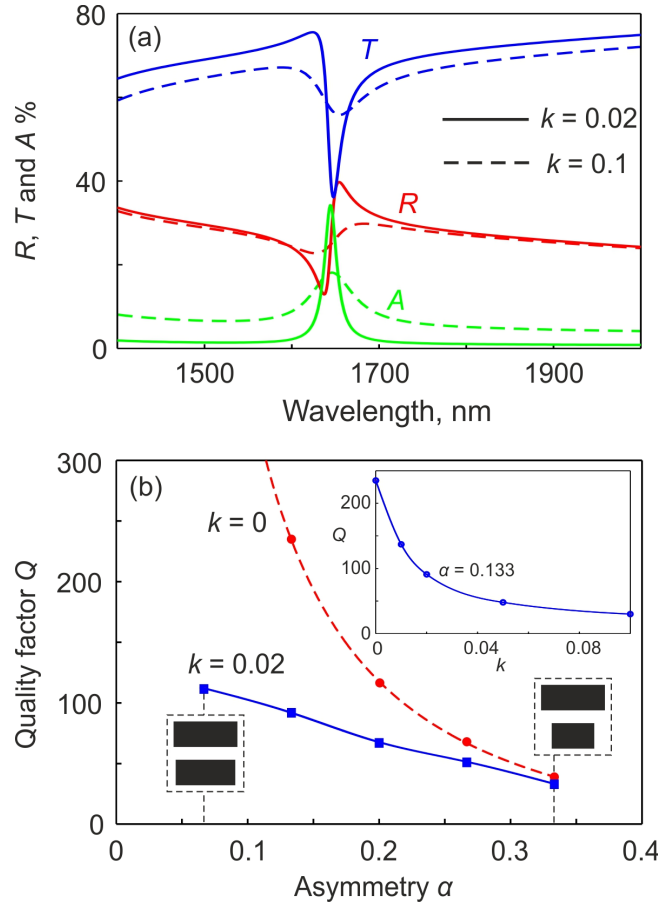


Fig. 5. The impact of absorption loss and asymmetry on dielectric metamaterial trapped mode resonance quality. (a) Simulated transmission, reflection and absorption spectra for the same metamaterial geometry [and the same x -polarized normally-incident illumination conditions] employed in Fig. 4 with non-zero values of the silicon absorption coefficient k : solid lines assume $n_{Si} = 3.5 + 0.02i$; dashed lines $n_{Si} = 3.5 + 0.1i$. (b) Resonance quality factor Q as a function of unit cell asymmetry α (defined as $\Delta L/L_2$ where ΔL is the difference between nanobar lengths L_1 and L_2 ; L_2 being the larger of the two) for zero and non-zero absorption levels as labeled. The inset shows Q as a function of absorption coefficient k at $\alpha = 0.133$ ($L_{1,2} = 650, 750$ nm).

Remarkably, for $n_{Si} = 3.5 + 0.02i$ the resonance retains a quality factor of ~ 91 and even at $n_{Si} = 3.5 + 0.1i$, $Q \sim 30$ - a value that would be considered good for a metal ASR metamaterial

in the VIS/NIR wavelength range [31]. Indeed, based on the measured parameters for PECVD films presented in Fig. 2(b) a silicon metamaterial resonant at $\lambda = 700$ nm, where $n_{Si} = 3.87 + 0.006i$, may present trapped mode resonances with Q values approaching 100. The experimental metamaterial sample presented here has a resonance quality factor of ~ 15 but crucially this is limited not by the intrinsic properties of the medium from which it is made (as is the case in metallic structures at visible and near-infrared wavelengths) but by the manufacturing process (as described above). Thus, with improvements in fabrication technique, visible and near-IR resonances with quality factors much higher than those typically achieved in conventional metallic metamaterials or plasmonic systems may be realized in dielectric structures, even in the presence of non-trivial losses.

As a point of interest, while the metamaterial considered here is not designed for the purpose of providing a strong magnetic *response*, i.e. a magnetic dipolar moment aligned with the incident magnetic field, the effective relative permittivity ϵ and permeability μ of such periodic arrays are intrinsically connected [32, 33] and a permittivity resonance is necessarily accompanied by a permeability anti-resonance as shown in Fig. 6.

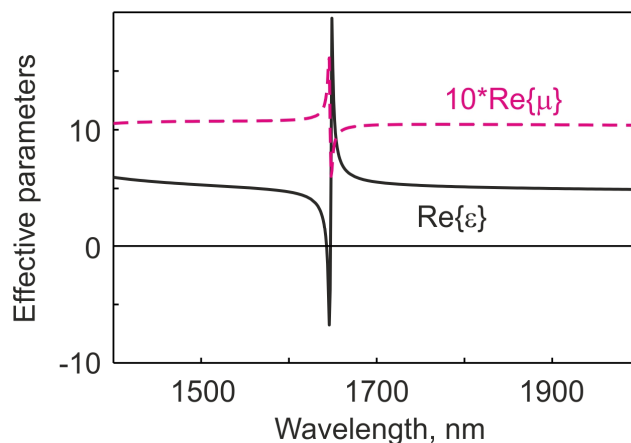


Fig. 6. Silicon metamaterial near-IR magnetic response. (a) Spectral dispersion of effective permittivity ϵ and permeability μ derived from simulated scattering data for the zero-loss asymmetric metamaterial model structure of Fig. 2(a) under normally incident x -polarized illumination [N.B. the amplitude of permeability is multiplied here by a factor of ten for visibility on the same scale as permittivity].

In summary, we have experimentally demonstrated a novel form of dielectric metamaterial composed of asymmetric silicon nano-bar pairs, which exhibits a sharp resonance in the near-IR wavelength range. The magnetic, trapped-mode nature of the resonance is illustrated in numerical simulations of electromagnetic response: The resonance is seen to depend critically on the existence of asymmetry between the two dielectric bars within the metamaterial unit cell and, while manufacturing imperfections (losses and inhomogeneous broadening) limit the resonance quality factor achieved in current experiential samples to values of order 15, simulations illustrate the potential for realization of VIS/NIR metamaterial resonances with Q -factors of several hundred using the silicon platform. Such structures open alternative paths to low-loss magnetism at optical frequencies and present new opportunities for controlling the output of quantum emitters [34, 35], realizing lasing spasers [36], and developing new kinds of opto-mechanically driven active metamaterials [37].

Acknowledgments

This work was supported by the Engineering and Physical Sciences Research Council [Project EP/G060363/1] (all authors), The Royal Society and the Ministry of Education, Singapore [grant MOE2011-T3-1-005] (NIZ), and the China Scholarship Council (JZ).